

Light and Electron Microscope Study on the Effect of Platelet-Rich Plasma in Induced Renal Ischaemia-Reperfusion Injury in the Renal Cortex of Adult Male Albino Rats

Samah M Ahmed¹, Abeer A Mahmoud¹, Ebtehal Z Hassen^{1*} and Rania R Abdel Kader²

¹Department of Histology and Cell Biology, Zagazig University, Egypt

²Department of Physiology, Faculty of Medicine, Zagazig University, Egypt

*Corresponding author: Ebtehal Z Hassen, Lecturer in Department of Histology and Cell Biology, Zagazig University, Egypt, Tel: 01001244853, E-mail: ebtehalzaid.81@gmail.com

Received date: September 11, 2018; Accepted date: September 20, 2018; Published date: September 27, 2018

Copyright: ©2018 Ahmed SM, et al. This is an open-access article distributed under the terms of the Creative Commons Attribution License, which permits unrestricted use, distribution, and reproduction in any medium, provided the original author and source are credited.

Abstract

Thirty four adult Wistar male albino rats were used in this study. They divided into three groups: Control, Ischemic-reperfusion (IR) and Platelet rich plasma treated groups. The levels of blood urea and serum creatinine were recorded. Renal reduced glutathione (GSH), superoxide dismutase (SOD), catalase (CAT) and malondialdehyde (MDA) were measured in the kidney homogenate. Samples from the kidney were processed for light and electron microscopic examination. A significant increase in the levels of blood urea and serum creatinine (mg/dl) was observed in IR group. Marked improvement in PRP group was detected. The activities of SOD, CAT and GSH levels in IR group decreased significantly as compared to controls. MDA level was high and significantly increased in IR group when compared with the control group. A significant increase of anti-oxidant enzyme activities and GSH levels and a significant decrease in MDA levels in PRP recipient group versus IR rats. Ischaemia-reperfusion injury causes congested glomerular capillaries, extravasation of RBCs. Some sections in IR group showed shrunken glomerulus with wide Bowman's space. Some tubular cells had pyknotic nuclei and others had intraluminal casts. PRP treated group showed marked improvement in their histological structure of renal cortical tissue. Masson trichrome stained sections of IR group showed increase in the collagen fibers and returned nearly as the control group in PRP treated group. PAS stained sections of IR group revealed strong positive reaction at the basal lamina of the tubular cells and the brush border of PCTs that returned as the control group in PRP treated group. Strong positive immunoreaction for caspase-3 in cytoplasm of renal tubules of the IR group, while PRP treated group revealed weak reaction. Our study found that ischemia-reperfusion injury causes deterioration of the kidney function and histological changes in the structure of renal cortex which were improved by PRP application.

Keywords Ischemia-reperfusion injury; Platelet-rich plasma; Rat kidney

Introduction

Ischaemia-reperfusion injury (IRI) is the reduction of blood supply to an organ followed by restoration of the blood flow and re-oxygenation. This condition triggers the damage of tissue by initiating an inflammatory process including reactive oxygen species (ROS), cytokines and leukocyte activation [1]. Renal ischemia reperfusion injury is the major cause of acute renal failure. It is often presented with conditions as renal transplantation, partial nephrectomy, renal trauma, hypovolaemia, sepsis, dehydration, tubular necrosis, shock with multi organ failure and surgical procedures that require renal artery occlusion for a long time [2]. It causes renal epithelial cell death and contributes to the delayed recovery of kidney function. Chronic renal hypoxia is an important mechanism in the development of tubulointerstitial fibrosis and progression of chronic renal disease [3].

PRP is an autologous derivative of the whole blood which has an important regenerative role in medicine. PRP is a source of growth factors as hepatocyte growth factor (HGF), insulin like growth factor-1 (IGF-1), adenosine diphosphate (ADP), adenosine tri-phosphate (ATP), and epidermal growth factor (EGF) liberated from α -granules and dense-granules of platelets that promote tissue repairing and

improve fibrosis [4]. These growth factors are released locally up to three weeks after application. Platelet derived growth factor (PDGF) encourage the formation of Type I collagen and promotes angiogenesis, transforming growth factor beta 1 (TGF- β 1) stimulates the proliferation and differentiation of mesenchymal stem cells and the synthesis of Type I collagen [5]. Autologous PRP is biocompatible and safe, assuming no contamination occurs during processing. Therefore, for clinical use, no special considerations concerning the antibody formation or risk of infection from donor are needed [6]. The administration of exogenous growth factors enhances renal tubule cell regeneration and accelerates the recovery of renal function. Some studies demonstrated that hepatocyte growth factor (HGF) stimulates regeneration of renal tubular cells which leads to the repair of kidney structure and function after damage. Therefore, PRP is as a natural cocktail of GFs which may enhance regeneration and functional recovery in kidney injuries [7]. So, the aim of this study was to evaluate the role of PRP in the improvement of renal ischemic reperfusion injury in adult male albino rats biochemically and histologically.

Materials and Methods

Drugs and chemicals

PRP preparation: PRP preparation was produced at the pharmacology department, faculty of medicine, Zagazig University.

Rats were anaesthetized with intraperitoneal injection of pentobarbitone sodium 60 mg/kg body weight, 2 ml of blood will be collected under aseptic technique from the retro-orbital plexus using capillary tubes initially dipped in 3.2% of sodium citrate, then collected into tubes containing 0.3 ml of the anticoagulant. Double centrifugation method was done for the collected blood which resulted in 3 different density compartments; the inferior layer contained red blood cells, the middle layer contained a buffy coat of white blood cells, and the superior layer contained plasma. The plasma will be pipetted and the portion just above a buffy coat will be obtained without disturbance of a buffy coat. The plasma will be centrifuged again at 2000 RPM for 10 minutes. This resulted in 2 parts: The top consisted of platelet-poor plasma (PPP) and the bottom consisted of platelet button. Part of the PPP will be discarded and part will be remained in the tube along with platelet button which then gently agitated to stimulate platelets re-suspension. This procedure will be resulted in the production of platelet-rich plasma (PRP). For confirmation of the platelet concentration, 80 μ L of the PRP sample will be counted in an automatic apparatus to verify that the platelet count was greater than 1,000,000/ μ L [8].

Animals

Thirty four adult Wistar male albino rats weighing (200-220 gm) were purchased from the Breeding Animal House, Faculty of Medicine, Zagazig University, Zagazig, Egypt. They were housed under standard laboratory conditions at room temperature. They were maintained on standard laboratory food and water ad libitum throughout the period of the experiment. All experimental procedures were approved and carried out in accordance with the guidelines of the Institutional Animal Care and Use Committee accepted by Faculty of Medicine, Zagazig University, Zagazig, Egypt.

Experimental design

Group I (Control group): Included fourteen rats that were equally subdivided into two subgroups

Subgroup Ia: Rats received no treatment.

Subgroup Ib (sham operated group): Rats were underwent identical surgical procedures as group II without bilateral renal clamping.

Rats of all subgroups were sacrificed with their corresponding experimental groups.

Group II: [Ischemia - Reperfusion treated group (IR group)]: Included ten animals that were anesthetized with intraperitoneal ketamine 50 mg/kg. A midline laparotomy was performed, both kidneys were located, and the renal pedicles, containing the artery, vein, and nerve supplying each kidney, were carefully isolated. Rats were allowed to stabilize for 45 min before subjected to bilateral renal pedicles clamping [9]. Once reperfusion commenced the artery clips were removed. The occlusion verified visually by a change in the colour of the kidneys to a paler shade and reperfusion by a blush [10].

Group III: (PRP treated group): Ten rats were subjected to surgical procedures as group II. Twenty four hours after IR injury, rats were anesthetized by sodium phenobarbital (50 mg/kg IP) and right and left abdominal incisions were performed. The right and left kidneys were exposed, and activated PRP was directly injected into the kidneys. Five subscapular punctures were done to distribute the activated PRP equally over the renal surface [2]. Rats of this group were sacrificed after two week from PRP injection. At the end of the experiment, rats

were anaesthetized with intraperitoneal injection of pentobarbitone sodium 60 mg/kg body weight. A midline incision was done on the anterior aspect of the chest, sternocostal junctions were cut, blood samples were collected from the abdominal aorta and the serum was harvested and stored at -20°C for assessment of kidney function tests. Rats were sacrificed and the kidneys were immediately isolated and specimens from the kidneys were collected. One half of the specimens were kept at -80°C for renal tissue parameter estimations. The other half was fixed in 10% neutral buffered formalin and processed for preparation of paraffin sections for histological study: (Hematoxylin and Eosin) [11], Masson trichrome [12] and PAS stains [12]. Immunohistochemical analysis for (caspase-3) [13] was also detected. For ultrastructural study, specimens were immediately fixed in 2.5% phosphate-buffered glutaraldehyde (pH 7.4). Thereafter, they were postfixed in 1% osmium tetroxide in the same buffer at 4°C, dehydrated, and embedded in epoxy resin [14].

Methods

Biochemical study

Blood urea and serum creatinine levels were measured for all rats. Measurements were estimated by conventional colorimetric method using Quanti Chrom TM assay kits.

Anti-oxidant status in kidney homogenate: Kidney specimens were homogenized in 100 mM tris-HCl (pH 7.4) and centrifuged at 12,000 \times g at 4°C. The supernatant was used for the estimation of renal anti-oxidant parameters including reduced glutathione (GSH), superoxide dismutase (SOD) activity and catalase activity (CAT). Renal GSH, SOD and CAT were measured by colorimetric methods following the manufacturer's instructions of the kits obtained from (Biodiagnostic, Cairo, Egypt).

Lipid peroxidation assay

Malondialdehyde (MDA), as a marker of lipid peroxidation, was measured colorimetrically in kidney homogenate with the use of a commercially available kit (Biodiagnostic, Cairo, Egypt). Thiobarbituric acid reacts with MDA in acidic medium to form thiobarbituric acid product, and the absorbance of the resultant product can be measured at 534 nm.

Histological study

Paraffin sections (5 μ m thick) stained with (H&E) for examination of overall morphology and Masson trichrome stain for examination of collagen fibers and PAS stain for carbohydrates.

Immunohistochemical study

Immunohistochemical reactions were carried out using the avidin-biotin peroxidase complex (Dakocompany, Wiesentheid/Bavaria, Germany, Biotin Blocking System, Code X0590) method following the manufacturer's instructions 4 μ m serial sections of paraffin-embedded specimens were deparaffinized on charged slides. The sections were incubated in 0.1% hydrogen peroxide for 10 min to block the endogenous peroxidase activity and then incubated with the primary antibody. The primary antibody used for caspase-3 was ready-to-use rabbit polyclonal antibody (CAT-No. RB-3425-R2). The slides were incubated with the secondary anti-rabbit antibody versal kits (Zymed laboratories), diluted 1: 200 for 30 minutes, staining was completed by

incubation with chromogen, called diamiobenzidine (DAB). Mayer's hematoxylin was used as a counterstain [13].

Ultrastructural study

Semithin sections 1 μ m thick were stained with 1% toluidine blue for light microscopic examination. Ultrathin sections were stained with uranyl acetate and lead citrate, examined and photographed using (JEOL JEM -2100) Transmission Electron Microscope (Jeol Ltd, Tokyo, Japan) in Electron Microscope Research Unit, Faculty of Agriculture, Mansoura University, Egypt.

Morphometric study

The image analyzer computer system Leica Qwin 500 (Leica Ltd, Cambridge, UK) in the image analyzing unit of the Pathology department, Faculty of Dentistry, Cairo University, Cairo, Egypt, was used to evaluate the area percentage (area %) of the collagen fibers between kidney tubules in Mallory trichrome stained sections, area % of positive PAS stained sections and area% of positive immune reaction for caspase-3 using the immunostained sections. It was measured using the interactive measure menu. The area % and standard measuring frame of a standard area equal to 118476.6 mm² were chosen from the parameters measuring 10 readings from five sections from each rat of the randomly chosen five rats in each group. In each chosen field, the section of the renal cortex was enclosed inside the standard measuring frame; the areas where collagen fibers, PAS positive reaction and brown positive immune reaction for caspase-3 was masked by blue binary color to be measured. These measurements were obtained by total magnification \times 400 with the area % of collagen fibers, PAS positive reaction and the area % of positive immune reaction for caspase-3.

Statistical analysis

For all groups, the data were expressed as mean \pm SD ($X \pm SD$). The data obtained from the image analyzer and the biochemical data were subjected to SPSS program version 14 (Chicago, Illinois, USA). Statistical analysis using the one-way analysis of variance test was carried out. The results were considered statistically significant as P value was less than 0.05.

Results

Biochemical results

Significant increase in the blood urea and serum creatinine (mg/dl) levels in IR group as compared to the control group levels. Marked improvement of blood urea and creatinine levels in PRP group was observed. The activities of SOD, CAT and GSH levels in group 2 (IR group) decreased significantly as compared with the controls. MDA level was high and significantly increased in IR group when compared with the control group. We found a significant increase of anti-oxidant enzyme activities and GSH levels and a significant decrease in MDA levels in group 3 (PRP recipient group) versus IR rats (Table 1).

Parameters	Control	IR group	PRP group
Serum creatinine (mg/dl)	0.63 \pm 0.05	2.11 \pm 0.06*	0.75 \pm 0.03*#
Blood urea (mg/dl)	20.3 \pm 3.4	80.5 \pm 4.5*	28.6 \pm 3.1*#
CAT (U/mg protein)	9.4 \pm 0.5	4.3 \pm 0.3*	9.2 \pm 0.4#

SOD (U/mg protein)	46.2 \pm 3.8	25.3 \pm 2.4*	42.5 \pm 2.6#
GSH (mg/g tissue)	30.4 \pm 1.2	21.6 \pm 1.6*	26.3 \pm 1.7*#
MDA (nmol/mg protein)	9.5 \pm 0.8	13.8 \pm 0.7*	10.3 \pm 0.5#

Table 1: Renal function and oxidant and anti-oxidant parameters in studied groups. *P<0.05 when compared to Control group. # P<0.05 when compared to IR group.

Histological results

Histological examination of the control subgroups showed similar morphologic results. So, subgroup Ia was considered as the control group. H and E stained sections of the control renal cortex in adult male albino rats showed the renal corpuscles and different types of tubules. Each renal corpuscle had glomerulus (tuft of capillaries) enclosed by visceral and parietal layers of Bowman's capsule enclosing Bowman's space (Figure 1). The renal cortex of IR group showed congested glomerular capillaries, extravasation of RBCs and the renal tubules were noticed with luminal casts.

Some sections in IR group showed shrunken glomerulus with wide Bowman's space. Some tubular cells had dark stained nuclei and other tubules had intraluminal casts. In PRP treated group marked improvement in the histological structure of renal cortical tissue, the glomerulus is surrounded by visceral and parietal layers of Bowman's capsule enclosing the Bowman's space. Renal tubules were normal.

Masson trichrome stained sections of the control group showed minimal collagen fibers in the interstitium between renal tubules (Figure 2) that increase in the IR group and returned as the control group in PRP treated group. PAS stained sections of control renal cortex revealed strong positive reaction at the basal lamina of the tubular cells and the brush border of PCTs, markedly increased in IR group and returned as the control group in PRP treated group (Figure 3).

Immunohistochemical results

Immunohistochemical staining for caspase-3 revealed faint positive immunoreaction in the cytoplasm of renal tubules of the control group (Figure 4). Strong positive reaction in the cytoplasm of renal tubules in IR group was observed. Weak positive immunoreaction in the cytoplasm of tubules was detected in PRP treated group.

Ultrastructural results

Electron microscope examination of ultrathin sections of the control renal cortex revealed the podocyte foot processes. Glomerular capillaries were lined by fenestrated endothelium. Glomerular filtration barrier was formed of regular glomerular basement membrane, fenestrated endothelium and secondary foot processes with filtration slit membrane (Figure 5).

Sections from IR group showed distorted podocyte foot processes, glomerular filtration barrier and thickened glomerular basement membrane. In PRP treated group, renal barrier with podocyte foot processes, glomerular capillaries with fenestrated endothelium, and regular glomerular basement membrane were detected.

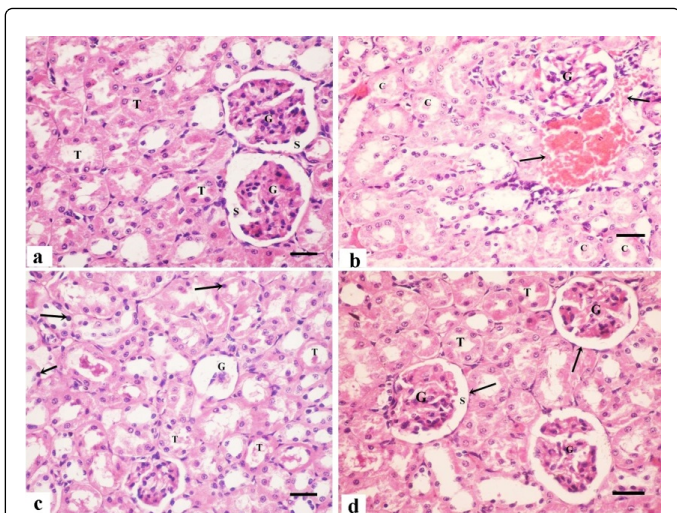


Figure 1: A photomicrograph of H&E stained sections of the control renal cortex showing the (a) Renal corpuscles (arrow) and tubules (T) with minimal interstitial tissue. Each renal corpuscle consists of glomerulus (G) that is surrounded by visceral and parietal layers of Bowman's capsule enclosing the Bowman's space (S). (b) Renal cortex of IR group showing glomeruli with congested capillaries (G), extravasation (arrow) and renal tubules containing casts (c) are also detected. (c) Some sections in IR group shows shrunken glomerulus (G) and tubules with intraluminal casts (T) and. (d) In PRP treated group, the glomerulus (G) is surrounded by visceral and parietal layers of Bowman's capsule enclosing the Bowman's space (S). Renal tubules (T) are normal. (H and E $\times 400$, Scale bar; 20 μm).

PRP group	16.32 \pm 15.3		
-----------	------------------	--	--

Table 4: Area % of caspase-3 immunoreaction in the different studied groups.

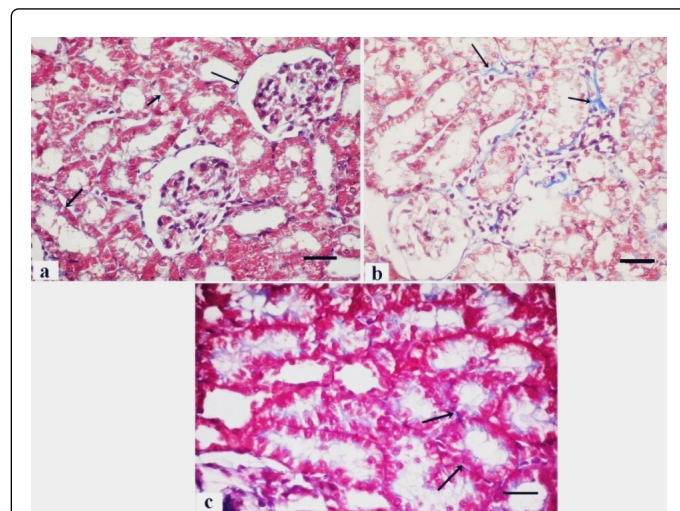


Figure 2: A photomicrograph of Masson trichrome stained sections of the control renal cortex (a) Showing minimal collagen fibers (arrow) in the interstitium between renal tubules. (b) Collagen fibers (arrow) increase in IR group. In PRP treated group, few collagen fibers (arrow) in the (c) Interstitium between renal tubules are noticed. (Masson trichrome $\times 400$, Scale bar; 20 μm).

Parameters	Mean \pm SD	F	P-value
Control group	12.08 \pm 0.02	76.821	<0.01*
IR group	22.341 \pm 0.03		
PRP group	13.016 \pm 0.01		

Table 2: Area % of collagen fibers in the different studied groups.

Parameters	Mean \pm SD	F	P-value
Control group	1.14 \pm 0.02	531.21	<0.001**
IR group	0.37 \pm 0.03		
PRP group	1.641 \pm 0.01		

Table 3: Area % of PAS reaction in the different studied groups.

Parameters	Mean \pm SD	F	P-value
Control group	14.95 \pm 13.2	111.03	<0.01*
IR group	36.11 \pm 18.1		

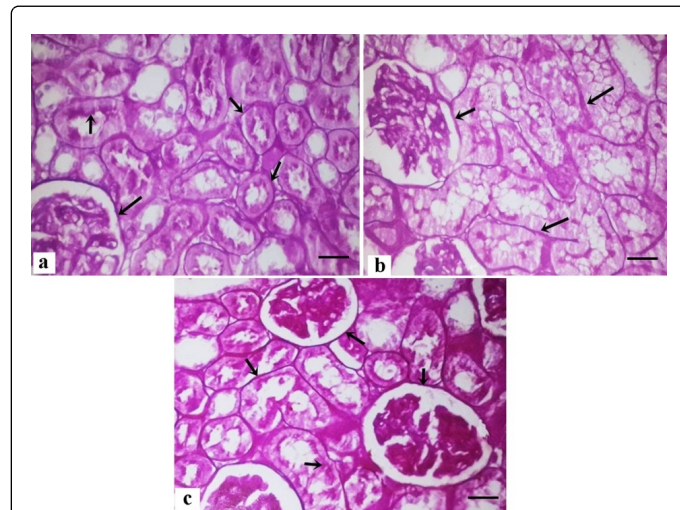


Figure 3: (a) A photomicrograph of PAS stained sections of the control renal cortex reveals strong positive reaction (arrow) at the basal lamina of the tubular cells and the brush border of PCTs. (b) This reaction (arrow) is markedly increased in IR group (c) PRP treated group showing strong positive reaction (arrow) at the basal lamina of the tubular cells and the brush border of PCTs. (PAS $\times 400$, Scale bar; 20 μm).

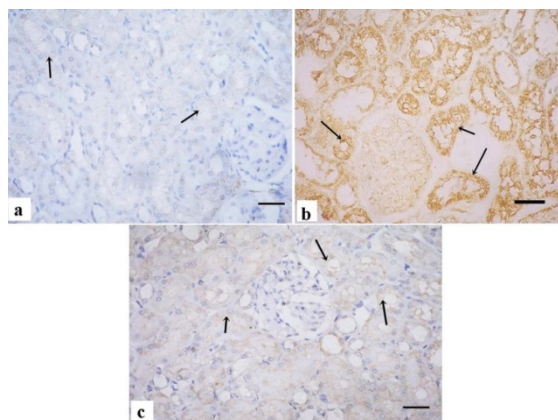


Figure 4: Immunohistochemical staining for caspase-3 reveal faint positive reaction. (a) (Arrow) in the cytoplasm of renal tubules of the control group. (b) Strong positive reaction in the cytoplasm of renal tubules in treated group is observed (arrow) in IR group. (c) In PRP treated group showing weak positive immunoreaction (arrow) in the cytoplasm of renal tubular cells. (Immunoperoxidase technique $\times 40$, Scale bar; 20 μm).

Electron microscopic examination of ultrathin sections of the control renal cortex showed the proximal convoluted tubular cells with euchromatic nuclei, luminal microvilli and apical pinocytotic vesicles. Basal infoldings and basal mitochondria were also noticed (Figure 6). IR group showed irregular basal infoldings, intracytoplasmic vacuolation and electron dense granules. Wide intercellular spaces, and apical microvilli were also noticed. Proximal convoluted tubular cells of PRP group showed euchromatic nuclei, closely packed apical microvilli, apical pinocytotic vesicles, basal mitochondria and basal infoldings. Electron microscopic examination of ultrathin sections of the control renal cortex showed the distal convoluted tubular cells with euchromatic nuclei, basal infoldings and basal mitochondria were detected. IR group showed irregular mitochondrial distribution, wide intercellular spaces and irregular basal infoldings (Figure 7). Distal convoluted tubular cells of PRP group showed euchromatic nuclei, regular basal mitochondria and basal infoldings.

Histo-morphometric and statistical results

Statistically significant increase in the mean area% of collagen fibers was detected in IR group as compared to the control and PRP treated groups. There were no statistically significant difference between Control group and PRP treated group (Table 2). Highly statistically significant decrease in the mean area % of PAS reaction was detected in IR group as compared to the control and PRP treated groups. No statistically significant difference between the control group and PRP treated group (Table 3). Statistically significant increase in the mean area% of caspase-3 immunoreaction was detected in IR group as compared to the control and PRP treated groups. No statistically significant difference between the control group and PRP treated group (Table 4).

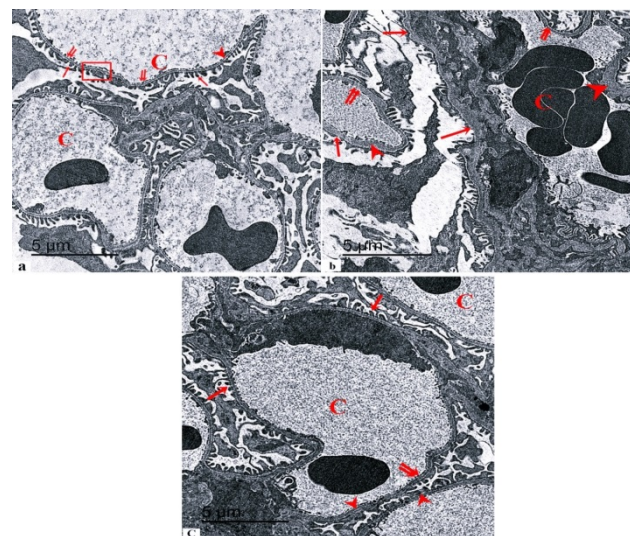


Figure 5: Electron microscope examination of ultrathin sections of the control: (a) Renal cortex showing glomerular capillaries (C) lined by fenestrated endothelium (double arrow). Glomerular filtration barrier (rectangle) is formed of regular glomerular basement membrane (arrow head), fenestrated endothelium (double arrow) and podocyte secondary foot processes (arrow) with filtration slit membrane. (b) Sections from IR group showing distorted podocyte foot processes (arrow), congested glomerular capillaries (C) with distorted endothelium (double arrow) and thickened glomerular basement membrane (arrow head). (c) In PRP treated group, renal barrier with podocyte foot processes (arrow), glomerular capillaries (C) with fenestrated endothelium (double arrow), and regular glomerular basement membrane (arrow head) are detected. (TEM, Scale bar; 5 μm).

Discussion

Many studies have been performed on PRP as a means of restoring or protecting various tissues, with generally good results; however, it is believed that there are few such studies in the field of urology.

In the current study, significant increase in the mean values of blood urea and serum creatinine levels in IR group. The activities of SOD, CAT and GSH levels in IR group decreased significantly as compared with the controls. MDA level was high and significantly increased in IR group when compared with the control group. We found a significant increase of anti-oxidant enzyme activities and GSH levels and a significant decrease in MDA levels in PRP recipient group versus IR rats. Spek [15] concluded that ROS post ischemic reperfusion results in lipid peroxidation which increase permeability of renal tubular cell membranes may lead to a loss of transport functions. Bonventre and Yang [16] found that increased production of reactive oxygen species (ROS) and induction of pro-inflammatory cytokines are important constituent in the acute tubular necrosis post ischemic reperfusion injury. Devarajan [17] added that lack of oxygen during ischemia leads to suppression of mitochondrial oxidative phosphorylation resulting in impaired ATP synthesis and decrease activity of cellular energy-dependent processes which could contribute to cell death. ATP depletion stops pumping calcium out of the cell therefore calcium accumulate in the cell causing cellular toxicity.

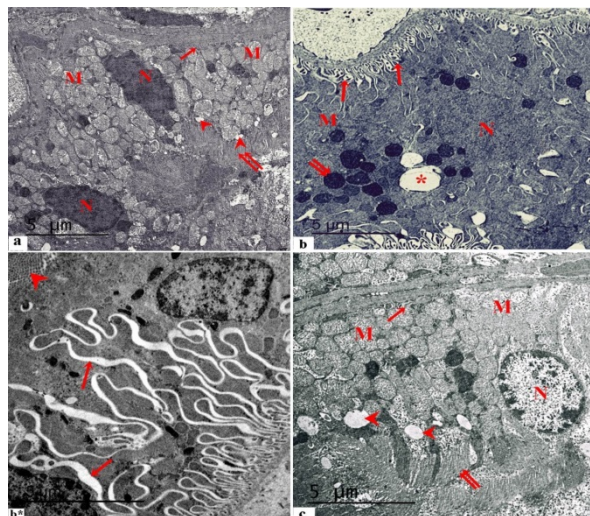


Figure 6: Electron microscopic examination of ultrathin sections of the control. 6a: Renal cortex showing the proximal convoluted tubular cells with euchromatic nuclei (N), luminal microvilli (double arrow) and apical pinocytotic vesicles (arrow head). Basal infoldings (arrow) and basal mitochondria (M) are also noticed. 6b: IR group showed irregular basal infoldings (arrow), intracytoplasmic vacuolation (*) and electron dense granules (double arrow). In the same group, wide intercellular spaces (arrow), and apical microvilli (arrow head) are also noticed. 6c: Proximal convoluted tubular cells of PRP group showed euchromatic nuclei (N), closely packed apical microvilli (double arrow), apical pinocytotic vesicles (arrow head), basal mitochondria (M) and basal infoldings (arrow). (TEM, Scale bar; 5 μ m).

In the present work, H and E stained sections of IR group showed congested glomerular capillaries, extravasation of RBCs, shrunken glomeruli with wide Bowman's space and luminal casts in the renal tubules. Some sections revealed tubular cells with dark stained nuclei. These histological changes were in accordance with Rao et al. [18] who founded also focal tubular dilation, flattening and attenuation of the epithelium, loss of the luminal brush border, apoptotic tubular cells, luminal necrotic debris and loss of renal parenchyma with ghost outlines of cells and structures with sharp demarcation from the adjacent viable tissue.

In the present study, Masson trichrome stained sections of IR group showed increase in collagen fibers in the interstitium. While PRP treated group showed diminish in collagen fibers in the interstitium between renal tubules. Statistically, there was significant increase in the mean area% of collagen fibers which detected in IR group as compared to Control and PRP treated groups. These findings are in agreement with the results of Forbes et al. [19]. They found that a significant increase in the deposition of collagens IV and III in the tubulo-interstitium which resolved by 16 days post-ischaemia.

They claimed the increase in collagen III and IV observed for several factors, including increased denovo synthesis by fibroblasts, increased tubular synthesis, decreased collagenase production, and increased synthesis of collagenase inhibitors. This is supported by a strong correlation between the appearance of myofibroblasts and collagen IV. Yang et al. [20] attributed the improvement in PRP group

to depletion of leukocytes which improve post-ischaemic renal function and structure due to reduced infiltration of myeloperoxidase cells, which was associated with decreased apoptosis, caspase-3 activity, inflammation and fibrosis.

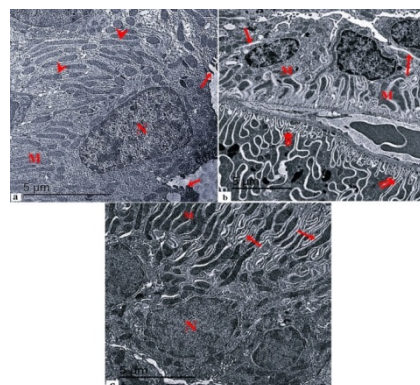


Figure 7: Electron microscopic examination of ultrathin sections of the control (a) Renal cortex showing the distal convoluted tubular cells with euchromatic nuclei (N), basal infoldings (arrow head) and basal mitochondria (M) are detected. Notice, apical microvilli (arrow). (b) IR group showed irregular mitochondrial distribution (M), wide intercellular spaces (arrow) and irregular basal infoldings (double arrow). (c) Distal convoluted tubular cells of PRP group showed euchromatic nuclei (N), regular basal mitochondria (M) and basal infoldings (arrow). (TEM, Scale bar; 5 μ m).

Examination of PAS stained sections of renal cortex from IR group revealed strong positive reaction at the basal lamina of the tubular cells and the brush border of PCTs. This finding explained by Shimizu et al. [21] who stated that reperfusion injury results in anoxia, leading to large amounts of cell adhesion molecules and lipid peroxidation, later resulting in possible necrosis and apoptosis. In the current study, strong positive immunoreaction for caspase-3 in cytoplasm of renal tubules of the IR group, while PRP treated group revealed weak reaction.

These findings were confirmed statistically, highly significant increase in area % of caspase-3 immunoreaction in cytoplasm of renal tubules of IR group as compared to the control group and PRP+IR group. Such finding was in agreement with Yang et al. [22]. They stated that, caspase-3 plays an important role in the execution of apoptosis, which modifies the progression of chronic I/R injury, and this may be a result of the divergent effects of different immunosuppressants as well. Guan et al. [23] attributed the improvement in PRP treated group to the transforming growth factor (TGF- β 1) which increases antiapoptotic Bcl-2 expression, maintains epithelial homeostasis and protects renal cells from apoptosis. Electron microscopic examination of the ultrathin sections from the renal cortex of IR group revealed distorted podocyte foot processes, glomerular filtration barrier and GBM.

PCT cells appeared with distorted mitochondria, microvilli and irregular basal infolding and wide intercellular spaces. DCT cells had irregular mitochondrial distribution and irregular basal infoldings. Similar improvement founded by Sekerci et al. [24]; who reported that PRP exerts protective effects on testicular tissues against I/R by inhibiting neutrophil infiltration and oxidative stress and increasing antioxidant defence.

In the current study, H and E stained sections of PRP treated group showed improvement in the histological structure of renal glomeruli and renal tubules and also improvement of kidney function which confirmed by ultrastructural findings and similar improvement was observed in Ischemia/Reperfusion Injury in rat ovary by Bakacak et al. [25] and Hargrave et al. [26].

They stated that PRP is effective for the prevention of ischemia and reperfusion damage in rat ovary and improve electrical and mechanical function of the heart *via* altered mitochondrial function and reduced apoptosis. Oh et al. [27] attributed the protective effect of PRP to its lack in surface immunogenic antigens, and thus allergic reactions are not of great concern. He et al. [28] stated that several growth factors, mainly epidermal growth factor (EGF), Insulin-like growth factor (IGF), Transforming growth factor (TGF- β 1) are released during renal ischemia-reperfusion. EGF is a strong promoter of growth in the renal tubular cells that attenuates tubular necrosis.

All of these growth factors are known to be released by PRP, so it could be expected that the application of PRP to an ischaemic kidney would improve its recovery. Liu et al. [29] stated that Vascular endothelial growth factor (VEGF) protects peritubular endothelium, induces the proliferation of tubular epithelial cells, promotes angiogenesis and accelerates renal recovery after ischaemia. In contrast to our finding, reported that PRP application McCarrel et al. [30] worsen the kidney instead of regenerating it. They claimed this to the release of cytokines and other proinflammatory agents, along with growth factors from injected platelets.

Conclusion

In conclusion, our study found that ischemia reperfusion injury causes histological damage of structure of renal cortex and deterioration of kidney function, which were improved by PRP application.

Conflicts of Interest

The authors report no conflicts of interest. The authors alone are responsible for the writing and content of the paper.

References

1. Sharfuddin AA, Molitoris BA (2011) Pathophysiology of ischemic acute kidney injury. *Nat Rev Nephrol* 7: 189-200.
2. Martín-Sole O, Rodo J, García-Aparicio L, Blanch J, Cusi V, et al. (2016) Effects of platelet rich plasma (PRP) on a model of renal ischemia reperfusion in rats. *PLoS One* 11: e0160703.
3. Rosenberge C, Rosen S, Heyman SN (2006) Renal parenchymal oxygenation and hypoxia adaptation in acute kidney injury. *Clin Exp Pharmacol Physiol* 33: 980-988.
4. Fortier LA, Barker JU, Strauss EJ, McCarrel TM, Cole BJ (2011) The role of growth factors in cartilage repair. *Clin Orthop Relat Res* 469: 2706-2715.
5. Ahmad Z, Howard D, Brooks RA, Wardale J, Henson FM, et al. (2012) The role of platelet rich plasma in musculoskeletal science. *JRSM short reports* 3: 40.
6. Li W, Enomoto M, Ukegawa M, Hirai T, Sotome S, et al. (2012) Subcutaneous injections of platelet-rich plasma into skin flaps modulate proangiogenic gene expression and improve survival rates. *Plast Reconstr Surg* 129: 858-866.
7. Matsumoto K, Nakamura T (2001) Hepatocyte growth factor: Renotropic role and potential therapeutics for renal diseases. *Kidney Int* 59: 2023-2038.
8. Pazzini JM, Nardi AB, Huppés R, Gering AP, Ferreira MG (2016) Method to obtain platelet-rich plasma from rabbits (*Oryctolagus cuniculus*). *Pesquisa Veterinária Brasileira* 36: 39-44.
9. Hussein AM, Abd-Elkhabir A, Abozahra A, Baiomy A, Ashamallah SA, et al. (2014) Pancreatic injury secondary to renal ischemia/reperfusion (I/R) injury: Possible role of oxidative stress. *Physiol Res* 63: 47-55.
10. Abogresha NM, Greish SM, Abdelaziz EZ, Khalil WF (2016) Remote effect of kidney ischemia-reperfusion injury on pancreas: Role of oxidative stress and mitochondrial apoptosis. *Arch Med Sci* 12: 252-262.
11. Bancroft J, Layton C (2013) *The Hematoxylin and eosin*. In: Suvarna SK, Layton C and Bancroft JD (ed). *Theory and Practice of histological techniques*. (7th edtn) Churchill Livingstone of Elsevier, Philadelphia, USA.
12. Drury RA, Wallington EA (1980) *Carlton's histological techniques*. (5th edtn). Oxford: Oxford University Press, USA.
13. Ramos-Vara JA, Kiupel M, Baszler T, Bliven L, Brodersen B, et al. (2008) Suggested guidelines for immunohistochemical techniques in veterinary diagnostic laboratories. *J Vet Diagn Invest* 20: 393-413.
14. Glauert AM, Lewis PR (1998) *Biological specimen preparation for transmission electron microscopy*. (1st edtn) Portland Press, London.
15. Spek CA, Brüggemann LW, Borensztajn KS (2010) Protease-activated receptor 2 blocking peptide counteracts endotoxin-induced inflammation and ameliorates renal fibrin deposition in a rat model of acute renal failure. *Shock* 33: 339-340.
16. Bonventre JV, Yang L (2011) Cellular pathophysiology of ischemic acute kidney injury. *J Clin Invest* 121: 4210-4221.
17. Devarajan P (2005) Cellular and molecular derangements in acute tubular necrosis. *Curr Opin Pediatr* 17: 193-199.
18. Rao K, Sethi K, Ischia J, Gibson L, Galea L, et al. (2017) Protective effect of zinc preconditioning against renal ischemia reperfusion injury is dose dependent. *PLoS One* 12: e0180028.
19. Forbes JM, Hewitson TD, Becker GJ, Jones CL (2000) Ischemic acute renal failure: Long-term histology of cell and matrix changes in the rat. *Kidney Int* 57: 2375-2385.
20. Yang B, Jain S, Ashra SY, Furness PN, Nicholson ML (2006) Apoptosis and caspase-3 in long-term renal ischemia/reperfusion injury in rats and divergent effects of immunosuppressants. *Transplantation* 81: 1442-1450.
21. Shimizu S, Tsounapi P, Dimitriadis F, Higashi Y, Shimizu T, et al. (2016) Testicular torsion-detorsion and potential therapeutic treatments: A possible role for ischemic postconditioning. *Int J Urol* 6: 454-463.
22. Yang B, Hosgood SA, Harper SJ, Nicholson ML (2010) Leucocyte depletion improves renal function in porcine kidney hemoreperfusion through reduction of myeloperoxidase + cells, caspase-3, IL-1 β , and tubular apoptosis. *J Surg Res* 164: e315-324.
23. Guan Q, Nguan CY, Du C (2010) Expression of transforming growth factor-beta1 limits renal ischemia-reperfusion injury. *Transplantation* 89: 1320-1327.
24. Sekerci CA, Tanidir Y, Sener TE, Sener G, Cevik O, et al. (2017) Effects of platelet-rich plasma against experimental ischemia/reperfusion injury in rat testis. *J Pediatr Urol* 13: 317.
25. Bakacak M, Bostanci MS, Inanc F, Yaylali A, Serin S, et al. (2016) Protective effect of platelet rich plasma on experimental ischemia/reperfusion injury in rat ovary. *Gynecol Obstet Invest* 81: 225-231.
26. Hargrave B, Li F (2012) Nanosecond pulse electric field activation of platelet-rich plasma reduces myocardial infarct size and improves left ventricular mechanical function in the rabbit heart. *J Extra Corpor Technol* 44: 198-204.
27. Oh DS, Cheon YW, Jeon YR, Lew DH (2011) Activated platelet-rich plasma improves fat graft survival in nude mice: A pilot study. *Dermatol Surg* 37: 619-625.
28. He S, Liu N, Bayliss G, Zhuang S (2013) EGFR activity is required for renal tubular cell dedifferentiation and proliferation in a murine model of folic acid-induced acute kidney injury. *Am J Physiol Renal Physiol* 304: F356-366.

29. Liu F, Lou YL, Wu J, Ruan QF, Xie A, et al. (2012) Upregulation of microRNA-210 regulates renal angiogenesis mediated by activation of VEGF signalling pathway under ischemia/perfusion injury in vivo and in vitro. *Kidney Blood Press Res* 35: 182-191.
30. McCarrel TM, Minas T, Fortier LA (2012) Optimization of leukocyte concentration in platelet-rich plasma for the treatment of tendinopathy. *J Bone Joint Surg Am* 94: e143-151.